The Astrophysical Journal, 735:56 (5pp), 2011 July 1 doi:10.1088/0004-637X/735/1/56

A LAW FOR STAR FORMATION IN GALAXIES

Andrés Escala
Departamento de Astronomía, Universidad de Chile, Casilla 36-D, Santiago, Chile
and
Kavli Institute for Particle Astrophysics and Cosmology, Stanford University Physics Department/SLAC, 2575 Sand Hill Road MS 29, Menlo Park, CA 94025, USA
Received 2009 October 9; accepted 2011 April 14; published 2011 June 16

ABSTRACT

We study the galactic-scale triggering of star formation. We find that the largest mass scale not stabilized by rotation, a well-defined quantity in a rotating system and with clear dynamical meaning, strongly correlates with the star formation rate in a wide range of galaxies. We find that this relation can be understood in terms of self-regulation toward marginal Toomre stability and the amount of turbulence allowed to sustain the system in this self-regulated quasi-stationary state. We test such an interpretation by computing the predicted star formation rates for a galactic interstellar medium characterized by a lognormal probability distribution function and find good agreement with the observed relation.

Key words: galaxies: formation – galaxies: ISM – galaxies: star formation – instabilities

1. INTRODUCTION

Observations of normal spiral galaxies by Schmidt (1959) first suggested that their star formation rates (SFRs) scale with their global properties. This relation was extended to other galaxies with higher SFRs, such as the nuclear regions of spiral galaxies and ultra-luminous infrared galaxies (ULIRGs) by Kennicutt (1998). These observations have led to an empirical law for star formation, often called the Kennicutt–Schmidt (KS) law,

$$\dot{\Sigma}_{\rm star} \propto \Sigma_{\rm gas}^{1.4}, \quad (1)$$

where $\Sigma_{\rm gas}$ and $\dot{\Sigma}_{\rm star}$ are the gas surface density and SFR per unit area, respectively.

Since star formation is a local process that happens on subparsec scales, the correlation with galactic-scale (>1 kpc) quantities, such as averaged $\Sigma_{\rm gas}$, suggests the existence of a physical connection between galactic and subparsec scales. Motivated by the observed KS law, several authors have tried to find a scenario in which a global/large scale property of galaxies could trigger and/or regulate star formation (Quirk 1972; Wyse 1986; Kennicutt 1989; Elmegreen 2002; Li et al. 2005). The KS law may also be explained in terms of processes that are primarily local, within star-forming clouds (e.g., Krumholz et al. 2009 and references therein).

From the study of gravitational instabilities in disks, the "turbulent" Toomre parameter $Q_{\rm turb} \equiv v_{\rm turb}^{\rm rms}\kappa/\pi G\Sigma_{\rm gas}$ (or related parameters such as the star formation threshold $\Sigma_{\rm crit}$; Kennicutt 1989) arises as a natural candidate for a key triggering parameter. However, the average $Q_{\rm turb}$ in a galaxy is observed to be close to 1, in galaxies ranging from local spirals (Martin & Kennicutt 2001) to starbursts such as ULIRGs (Downes & Solomon 1998). Since observed values of $Q_{\rm turb}$ (or $\Sigma_{\rm gas}/\Sigma_{\rm crit}$) range over at most a factor of a few, the observed range in SFRs per unit area of seven orders of magnitude is difficult to explain solely in terms of this threshold. Therefore, further investigation is required to determine what controls the SFRs on galactic scales.

An important point not generally addressed is that a disk at the condition of marginal Toomre stability can have a range of possible self-regulated states. For example, the nuclear disk in a starburst with $Q \sim 1$ is much more turbulent than the disk of a normal spiral galaxy with $Q \sim 1$. The goal of this work is to study which galactic property triggers this more turbulent behavior for some galaxies and why their SFRs can be orders of magnitude higher than in more "quiescent" spiral galaxies.

This work is organized as follows. We first review gravitational instability analysis in order to introduce the largest scale not stabilized by rotation, followed in Section 2 by a discussion of the correlation found between this largest scale and the SFR. Section 3 presents a physical interpretation of the correlation found in terms of self-regulation due to feedback processes. In Section 4, we test such an interpretation by comparing predictions against the observed SFRs. Finally, in Section 5, we summarize the results of this work.

2. THE MAXIMUM SCALE NOT STABILIZED BY ROTATION

In order to introduce the largest unstable length scale in galactic disks, we first review some standard results from gravitational instability analysis (Toomre 1964; Goldreich & Lynden-Bell 1965). For one of the simplest cases of a differentially rotating thin sheet or disk, linear stability analysis yields the dispersion relation for small perturbations (Binney & Tremaine 2008) $\omega^2 = \kappa^2 - 2\pi G\Sigma_{\rm gas}|k| + k^2C_{\rm s}^2$, where $C_{\rm s} = \sqrt{dP/d\Sigma}$ is the sound speed, Σ is the surface density, and κ is the epicyclic frequency given by $\kappa^2(R) = R\frac{d\Omega^2}{dR} + 4\Omega^2$ (Ω being the angular frequency). The system becomes unstable when $\omega^2 < 0$, which is equivalent to the condition $Q < 1$, where Q is the Toomre parameter and is defined as $C_{\rm s}\kappa/\pi G\Sigma_{\rm gas}$. In such a case there is a range of unstable length scales limited on small scales by thermal pressure (at the Jeans length $\lambda_{\rm Jeans} = C_{\rm s}^2/G\Sigma_{\rm gas}$) and on large scales by rotation (at the critical length set by rotation, $\lambda_{\rm rot} = 4\pi^2G\Sigma_{\rm gas}/\kappa^2$). All intermediate length scales are unstable, and the most rapidly growing mode has a wavelength $2\lambda_{\rm Jeans}$ (Binney & Tremaine 2008; Escala & Larson 2008).

The maximum unstable length scale in a disk, $\lambda_{\rm rot}$, is a robust quantity because it depends only on the surface density and epicyclic frequency of the disk and not on smaller scale physics. Such a length scale has an associated characteristic mass, defined as equal to $\Sigma_{\rm gas}(\lambda_{\rm rot}/2)^2$, which can be expressed

as

$$M_{\rm rot} = \frac{4\pi^4 G^2 \Sigma_{\rm gas}^3}{\kappa^4}. \quad (2)$$

On the other hand, due to the complex structure and dynamics of the real interstellar medium (ISM) in galaxies, which cannot be described by a simple equation of state, there is not a well-defined Jeans length at intermediate scales. Therefore, there is no real lower limit on the sizes of the self-gravitating structures that can form until the thermal Jeans scale is reached in molecular cloud cores (Escala & Larson 2008).

The combination of the observed correlations of SFRs with galactic properties, and the fact that this largest scale not stabilized by rotation is the only well-defined galactic scale in the gravitational instability problem, is our motivation for exploring a possible link between SFR and this characteristic galactic scale.

2.1. The Law

In order to test the existence of a link between the largest scale not stabilized by rotation and the SFR in galaxies, we will check whether the mass scale defined by rotation (Equation (2)) correlates with the SFR. For a rotationally supported system, the average of this mass scale can be expressed in terms of quantities such as the gas mass and gas fraction (Escala & Larson 2008):

$$M_{\rm rot} = 3 \times 10^7 M_\odot \frac{M_{\rm gas}}{10^9 M_\odot} \left(\frac{\eta}{0.2}\right)^2, \quad (3)$$

where $M_{\rm gas}$ is the gas mass in the disk and $\eta = M_{\rm gas}/M_{\rm dyn}$ is the ratio of the gas mass to the total enclosed dynamical mass within the gas radius (this varies from the disk radius for spiral galaxies to the radius of the nuclear starburst disk/ring in ULIRGs). This expression (Equation (3)) has the advantage that it reduces the scatter due to error propagation compared to the original formulation (Equation (2)).

In Figure 1, we plot the maximum mass scale not stabilized by rotation estimated from Equation (3) against the measured SFR (per unit area) in those galaxies. We plot normal spirals as star symbols, the nuclear gas in normal spirals as filled circles, and ULIRGs as open circles. For the computation of $M_{\rm rot}$, we have considered only molecular gas masses and molecular gas fractions. This is because molecular gas should be intimately related to the SFR because it is this gas which eventually forms the stars in giant molecular clouds. Error bars displayed in Figure 1 show uncertainties estimated by error propagation from the uncertainties found in the literature.

The information for each data point plotted in Figure 1 is listed in Table 1, together with a list of references to the works in the literature from which the values were taken. For the spiral galaxies, $\dot{\Sigma}_\star$ is estimated from the Hα luminosity, the gas masses are estimated by the CO luminosity, and the dynamical masses are estimated using the method listed in Table 1. For the nuclear gas in normal spirals, the gas masses are estimated using the CO luminosity, the dynamical masses from rotation curves, and $\dot{\Sigma}_\star$ is estimated using the method listed in Table 1. Finally, for ULIRGs, $\dot{\Sigma}_\star$ is estimated from the far-infrared luminosity, gas masses are estimated from the CO luminosity, and dynamical masses are estimated using rotation curves.

Figure 1 shows a clear correlation between $M_{\rm rot}$ and the SFR per unit area, which supports the idea that this threshold mass has a relevant role in the triggering of star formation on galactic scales. The solid black line in Figure 1 shows a least-squares fit

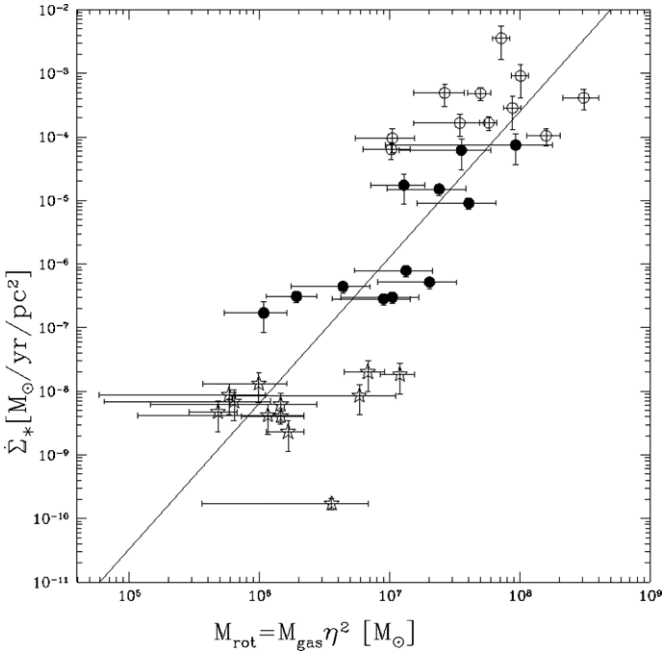

Figure 1. Star formation rate plotted against the critical mass scale defined by rotation $M_{\rm rot}$, estimated from Equation (3) using measured quantities in those galaxies. The open circles show data for nuclear starburst disks, the star symbols show for normal spiral galaxies, and the filled circles show for nuclear gas in spirals. The solid line corresponds to $\dot{\Sigma}_\star \propto M_{\rm rot}^{2.3}$.

to the points in the figure and corresponds to a star formation law of $\dot{\Sigma}_\star \propto M_{\rm rot}^{2.3}$, with a scatter of 0.21 dex. This relation has a level of scatter comparable to the typical scatter found for the KS law. Moreover, this is the only correlation of the SFR with a galactic quantity with a clear dynamical meaning in terms of stability analysis, and therefore with a clear role in the star formation problem.

In summary, the correlation between the SFR and the maximum unstable mass defined by rotation is indeed observed in galaxies over a range that spans almost eight orders of magnitude in SFR per unit area.

3. A PHYSICAL INTERPRETATION IN TERMS OF SELF-REGULATION

It is well established that galactic disks are globally observed to be in equilibrium, for galaxies ranging from local spirals (Martin & Kennicutt 2001) to starbursts such as ULIRGs (Downes & Solomon 1998) with measured Toomre Q parameters close to 1 in the case of a "turbulent" version of the Toomre parameter: $Q_{\rm turb} = v_{\rm turb}^{\rm rms}\kappa/\pi G\Sigma$, where $v_{\rm turb}^{\rm rms}$ is the observed velocity dispersion in the gas. This state close to stability ($Q_{\rm turb} \sim 1$) was first suggested by Goldreich & Lynden-Bell (1965) to be due to a self-regulation feedback loop; if $Q_{\rm turb} \gg 1$, in the absence of heating driven by instabilities the disk will cool rapidly and the system will eventually become unstable, while if $Q_{\rm turb} \ll 1$ then instabilities and star formation feedback will be so efficient that enough turbulence will be produced to "heat" the disk toward $Q_{\rm turb} \sim 1$.

While most galactic disks are close to marginal Toomre stability, some, such as nuclear disks in starbursts, can be much more turbulent than the disks of normal spiral galaxies. The reason is that although disks are all at $Q_{\rm turb} \sim 1$, they can have self-regulated states with different levels of turbulence ($v_{\rm turb}^{\rm rms}$). This can be easily visualized by considering that the

Table 1
Galaxy Physical Parameters

Galaxy	$\dot{\Sigma}_\star$ ($M_\odot$ yr^{-1} kpc^{-2})	M_{H_2} (10^9 $M_\odot$)	M_{dyn} (10^{10} $M_\odot$)	$\eta = \frac{M_{H_2}}{M_{dyn}}$	References
NGC6946	0.0132	3.3	19[a]	0.02	(1), (3)
NGC4419	0.00404	4	9[b]	0.044	(2), (4), (5)
NGC4535	0.00017	6.918	26.3[c]	0.0263	(2), (4), (6)
NGC5033	0.00229	6.708	37.1[b]	0.018	(1), (7), (8)
NGC4254	0.01995	13.427	51.6[b]	0.019	(1), (4), (9)
NGC7331	0.004677	4.94	21.5[a]	0.023	(1), (8), (10)
NGC4303	0.018197	10	25[a]	0.04	(1), (4), (11)
NGC4647	0.0069	2.63	14.6[c]	0.018	(1), (4), (6)
NGC4654	0.0087	3.236	20.88[c]	0.0155	(1), (4), (6)
NGC4321	0.00851	14.791	64.3[c]	0.023	(1), (4), (6)
NGC4501	0.006166	9.77	69.3[c]	0.0141	(1), (4), (6)
NGC4689	0.00417	3.09	13.8[c]	0.0224	(1), (4), (6)
NGC253	17.378[d]	0.14	0.04	0.35	(1), (12)
NGC1614	61.6595[d]	2	1.3	0.154	(1), (13)
NGC470	0.7892[e]	0.2	0.067	0.299	(14)
NGC4102[f]	9.06539[e]	0.8	0.3	0.26	(14)
NGC4102[g]	3.00654[e]	1.4	1.4	0.1	(14)
NGC3504[f]	1.50835[e]	0.8	0.4	0.2	(14)
NGC3504[g]	2.8349[e]	1.2	1.2	0.1	(14)
NGC4536	0.5175[e]	1.2	0.8	0.15	(14)
NGC3351	0.4421[h]	0.2	0.117	0.171	(14)
NGC3627	0.1698[d]	2	6	0.03	(1), (15), (16)
NGC6240	74.131[d]	3.1	1.55	0.2	(1), (17)
NGC5005	0.3107[i]	1.03	2	0.05	(2), (18)
IRAS00057	95.1	1.4	1.4	0.1	(19)
IRAS02483	63.6	1.9	2.235	0.085	(19)
IRAS10565	104.1	4	1.739	0.23	(19)
Mrk231	492	1.8	1.286	0.14	(19)
Arp193	487.1	2.6	1.625	0.16	(19)
Arp220 disk	166.5	3	1.875	0.16	(19)
Arp220 total	285.4	5.2	3.467	0.15	(19)
Arp220 west	3555.1	0.6	0.15	0.4	(19)
Arp220 east	905.7	1.1	0.314	0.35	(19)
IRAS17208	413.4	6.1	2.346	0.26	(19)
IRAS23365	164.8	3.8	3.455	0.11	(19), (20)

Notes.
[a] H I rotation curves.
[b] CO rotation curves.
[c] M_{dyn}–L_H relation.
[d] L_{FIR}.
[e] L_{RC}.
[f] @300 pc.
[g] @1300 pc.
[h] $L_{Br\gamma}$.
[i] $L_{H\alpha}$.

References. (1) Kennicutt 1998; (2) Komugi et al. 2005; (3) Crosthwaite & Turner 2007; (4) Young et al. 1996; (5) Kenney & Young 1989; (6) Decarli et al. 2007; (7) Pérez-Torres & Alberdi 2007; (8) Helfer et al. 2003; (9) Sofue et al. 2003; (10) Thilker et al. 2007; (11) Schinnerer et al. 2002; (12) Mauersberger et al. 1996; (13) Alonso-Herrero et al. 2001; (14) Jogee et al. 2005; (15) Reuter et al. 1996; (16) Warren et al. 2010; (17) Engel et al. 2010; (18) Sakamoto et al. 2000; (19) Downes & Solomon 1998; (20) Murphy et al. 1996.

condition $Q_{turb} \sim 1$ implies a mass scale of $M_{rot} \sim \frac{4\pi}{G\kappa}[v_{turb}^{rms}]^3$ using Equation (2). Since the epicyclic frequency κ varies only between Ω and 2Ω for centrally concentrated disks, in a disk supported vertically by turbulence ($\Omega^{-1} = R/v_{circ} \sim H/v_{turb}^{rms}$) it is straightforward to derive a mass scale of

$$M_{rot} \sim \frac{8\pi}{3G} H\left[v_{turb}^{rms}\right]^2 \quad (4)$$

for a median epicyclic frequency of $\kappa = 3/2\,\Omega$. Since the disk scale height H is a monotonically increasing function of v_{turb}^{rms} for a disk supported vertically by turbulence, the velocity dispersion of turbulent motions follows $v_{turb}^{rms} \propto M_{rot}^{\eta}$ with $\eta > 0$, for a disk with $Q_{turb} \sim 1$. Therefore, since some disks have a larger mass scale not stabilized by rotation M_{rot}, their large-scale conditions require that feedback processes produce more turbulence in order to achieve $Q_{turb} \sim 1$.

The existence of disks with self-regulated states of different v_{turb}^{rms} is particularly important because it is believed that turbulence has a role in enhancing and controlling star formation (Elmegreen 2002; Krumholz & McKee 2005; Wada & Norman

2007). In its simplest form (proposed by Elmegreen 2002), the SFR depends on the probability distribution function (PDF) of the gas density produced by galactic turbulence, which appears to be lognormal in simulations of turbulent molecular clouds and the ISM (Ballesteros-Paredes & Mac Low 2002; Padoan & Nordlund 2002; Kravtsov 2003; Mac Low et al. 2005; Wada & Norman 2007; Wang & Abel 2009). Moreover, numerous numerical studies support the fact that the dispersion of the lognormal PDF is determined by the rms Mach number of the turbulent motions (Vázquez-Semadeni 1994; Padoan et al. 1997; Padoan & Nordlund 2002; Federrath et al. 2008, 2010). Therefore, it is expected that the SFR in galaxies scales with the velocity dispersion of turbulent motions. From this we can infer, at least qualitatively, that a galaxy with a higher $M_{\rm rot}$ should have a higher star formation activity.

In summary, as the largest mass scale not stabilized by rotation $M_{\rm rot}$ increases for a given disk, its self-regulated state has an increasingly turbulent ISM ($v_{\rm turb}^{\rm rms} \propto M_{\rm rot}^{\eta}$ with $\eta > 0$, for $Q_{\rm turb} \sim 1$). A self-regulated state with higher $v_{\rm turb}^{\rm rms}$ (which itself controls and enhances star formation) implies higher star formation activity, and therefore the correlation between the critical mass scale defined by rotation and the SFR is expected.

4. GALACTIC SFR FOR AN ISM CHARACTERIZED BY A LOGNORMAL PDF

In order to quantify the arguments given above, in this section we will compute the predicted SFR for an ISM dynamically controlled by turbulence in which the rms velocity dispersion of turbulent motions $v_{\rm turb}^{\rm rms}$ is determined by $M_{\rm rot}$. We will follow an analysis analogous to Wada & Norman (2007), starting with the assumption that the density PDF of the multiphase ISM in a galactic disk can be represented by a single lognormal function:

$$f(\rho)d\rho = \frac{1}{\sqrt{2\pi}\sigma}\exp\left[-\frac{\ln(\rho/\rho_0)}{2\sigma^2}\right]d\ln\rho, \quad (5)$$

where ρ_0 is the characteristic density scale and σ is the dispersion of the lognormal PDF. Although there is evidence for deviations from a lognormal function in the tails of the density PDF (Scalo et al. 1998; Federrath et al. 2010), for simplicity we neglect any higher order correction.

If the star formation occurs only in regions whose density is higher than a critical value ($\rho > \rho_c$), the SFR per unit volume on a global scale is given by

$$\dot{\rho}_\star = \epsilon_c (G\rho_c)^{1/2} f_c \langle\rho\rangle_V, \quad (6)$$

where ϵ_c is the efficiency of star formation, $\delta_c = \rho_c/\rho_0$ is the critical density contrast for star formation, $\langle\rho\rangle_V = \rho_0 e^{\sigma^2/2}$ is the volume-average density, and $f_c = 0.5[1 - {\rm Erf}(\frac{\ln\delta_c - \sigma^2}{\sqrt{2}\sigma})]$ is the mass fraction of gas whose density is higher than ρ_c (for a derivation see Section 3 of Wada & Norman 2007). Numerous numerical studies have claimed that, in addition to the approximately lognormal form of the PDF, the dispersion σ is determined by the rms Mach number $\mathcal{M}_{\rm rms} = v_{\rm turb}^{\rm rms}/C_{\rm S}$, where $C_{\rm S}$ is the sound speed (Vázquez-Semadeni 1994; Padoan et al. 1997; Padoan & Nordlund 2002; Federrath et al. 2008, 2010). When a lognormal PDF is assumed, the σ–$\mathcal{M}_{\rm rms}$ relation can be expressed as (Padoan et al. 1997)

$$\sigma^2 = \ln\left(1 + b^2\,\mathcal{M}_{\rm rms}^2\right), \quad (7)$$

where b is a parameter that varies from 0.3 to 1 and depends, for example, on the compressive to solenoidal modes of the turbulence forcing (Federrath et al. 2010). Since the forcing mode (and therefore b) may vary across regions of the ISM (Federrath et al. 2010), and since the sound speed certainly does vary across the ISM, it is convenient for our analysis to define a volume-averaged, b-weighted, sound speed $\widetilde{C}_{\rm S} = \langle\frac{C_{\rm S}}{b}\rangle_{\rm V}$.

Using Equations (4), (6), and (7), we can write the SFR per unit area ($\dot{\Sigma}_\star = \dot{\rho}_\star\, H$) as

$$\dot{\Sigma}_\star = 1.72\times10^{-5}\frac{M_\odot}{{\rm pc}^2\ {\rm yr}}\epsilon_c\delta_c^{1/2}\left(\frac{\rho_0}{M_\odot\ {\rm pc}^{-3}}\right)^{3/2} \times\left[1 - {\rm Erf}\left(z\left(\delta_c,\, M_{\rm rot}\,H^{-1}\widetilde{C}_{\rm S}^{-2}\right)\right)\right]$$

$$\times\left[1.95\frac{H}{\rm kpc} + \left(\frac{\rm km\ s^{-1}}{\widetilde{C}_{\rm S}}\right)^2\frac{M_{\rm rot}}{10^6\ M_\odot}\right] \quad (8)$$

and

$$z\left(\delta_c,\, M_{\rm rot}\,H^{-1}\widetilde{C}_{\rm S}^{-2}\right) = \frac{\ln\delta_c - 2\ln\left(1 + \frac{3G}{8\pi}\frac{M_{\rm rot}}{H\widetilde{C}_{\rm S}^2}\right)}{2\left(\ln\left(1 + \frac{3G}{8\pi}\frac{M_{\rm rot}}{H\widetilde{C}_{\rm S}^2}\right)\right)^{1/2}}. \quad (9)$$

Figure 2 shows the comparison of the predicted correlation between $\dot{\Sigma}_\star$ and $M_{\rm rot}$ from Equation (8) against the data listed in Table 1, for several values for the model parameters ρ_0, ϵ_c, δ_c, and$\widetilde{C}_{\rm S}$. The thick solid lines in Figures 2(a)–(d) represent the predicted $\dot{\Sigma}_\star$ for model parameters $\rho_0 = 1\ M_\odot\ {\rm pc}^{-3}$, $\epsilon_c = 0.01$, $\delta_c = 10^3$, and $\widetilde{C}_{\rm S}$ equivalent to a temperature of 250 K. The other four curves in Figure 2(a) show variations in the predicted SFRs for $\rho_0 = 10^{-2}$, 10^{-1}, 10^{1}, and $10^{2}\ M_\odot\ {\rm pc}^{-3}$. The four curves in Figure 2(b) show SFRs for $\epsilon_c = 1, 10^{-1}, 10^{-3}$, and 10^{-4}. In Figure 2(c) the curves show SFRs for $\delta_c = 10, 10^2, 10^4$, and 10^5. Finally, the curves in Figure 2(d) show SFRs for $\widetilde{C}_{\rm S}$ equivalent to temperatures of $T = 25$, 75, 750, and 2500 K.

From Figure 2, it can be concluded that with a single set of parameters (thick solid lines) Equation (8) is able to successfully reproduce the whole correlation, in contrast with the analogous work of Wada & Norman (2007), which did not reproduce the KS law with a single set of parameters and relied on a variable star formation efficiency ϵ_c (between normal and starburst galaxies) in order to reproduce the observed data.

5. SUMMARY

In this paper, we have studied the role of the largest mass scale not stabilized by rotation in galactic disks in triggering star formation activity in galaxies.

We find that a relation between the largest mass scale not stabilized by rotation and the SFR is observed in galaxies ranging from ULIRGs to normal spirals. This relation has a level of scatter comparable to the KS law and is the only known correlation of the global SFR with a quantity with clear dynamical meaning in terms of stability analysis.

We give a physical interpretation for the existence of such a correlation in terms of self-regulation. In a given disk, as the largest mass scale not stabilized by rotation increases, its self-regulated quasi-stationary state has an increasingly turbulent ISM ($v_{\rm turb}^{\rm rms} \propto M_{\rm rot}^{\eta}$ with $\eta > 0$, for $Q_{\rm turb} \sim 1$). Therefore, the role of the critical mass scale in a disk is to define the amount of turbulence allowed to be in quasi-stationary equilibrium. Since a self-regulated state with higher $v_{\rm turb}^{\rm rms}$ enhances a higher star

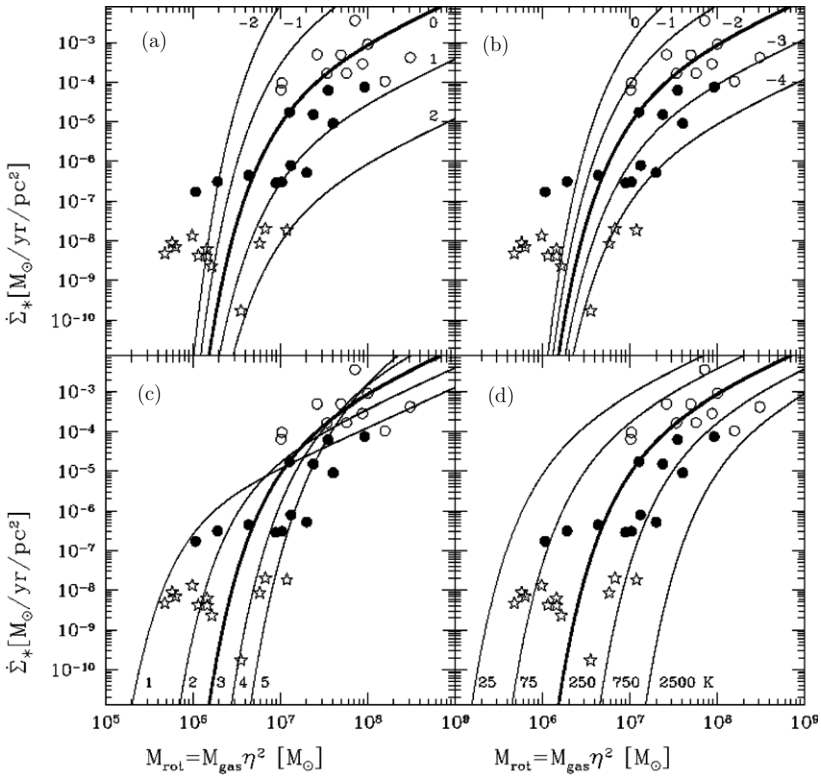

Figure 2. Predicted correlation between $\dot{\Sigma}_\star$ and $M_{\rm rot}$ from Equation (8) against the data listed in Table 1, for several values for the model parameters ρ_0, ϵ_c, δ_c, $\langle C_{\rm S}\rangle$. The thick solid lines in all figures show the model with $\rho_0 = 1\ M_\odot\ {\rm pc}^{-3}$, $\epsilon_c = 0.01$, $\delta_c = 10^3$, and $\widetilde{C}_{\rm S}$ equivalent to a temperature of 250 K. (a) The other lines show the variations in SFRs (per unit area) for $\log(\rho_0/M_\odot\ {\rm pc}^{-3}) = -2, -1, 0, 1,$ and 2. (b) The lines show SFRs for $\log\epsilon_c = 0, -1, -2, -3,$ and -4. (c) Curves show SFRs for $\log\delta_c = 1, 2, 3, 4,$ and 5. (d) Curves show SFRs for $\widetilde{C}_{\rm S}$ equivalent to temperatures of $T = 25$, 75, 250, 750, and 2500 K.

formation activity, we expect the existence of a correlation between the mass scale for global stability and the SFR.

We check the validity of this self-regulation scenario by computing the predicted SFR for an ISM dynamically controlled by turbulence in which the rms velocity dispersion of turbulent motions $v_{\rm turb}^{\rm rms}$ is determined by $M_{\rm rot}$. We find good agreement between the predicted and observed SFRs.

I thank Richard Larson for valuable comments on an early version of the draft, Catherine Vlahakis for proofreading this manuscript, and the referee, Brant Robertson, for a constructive report. I am indebted to Fernando Becerra for performing the error analysis and graphical display. I also acknowledge partial support from the Center of Excellence in Astrophysics and Associated Technologies (PFB 06), FONDECYT Iniciacion Grant 11090216, and from the Comite Mixto ESO-Chile.

REFERENCES

Alonso-Herrero, A., Engelbracht, C. W., Rieke, M. J., Rieke, G. H., & Quillen, A. C. 2001, ApJ, 546, 952
Ballesteros-Paredes, J., & Mac Low, M.-M. 2002, ApJ, 570, 734
Binney, J., & Tremaine, S. 2008, Galactic Dynamics (Princeton, NJ: Princeton Univ. Press)
Crosthwaite, L. P., & Turner, J. L. 2007, AJ, 134, 1827
Decarli, R., et al. 2007, MNRAS, 381, 136
Downes, D., & Solomon, P. M. 1998, ApJ, 507, 615
Elmegreen, B. G. 2002, ApJ, 577, 206
Engel, H., et al. 2010, A&A, 524, 56
Escala, A., & Larson, R. B. 2008, ApJ, 685, L31
Federrath, C., Klessen, R. S., & Schmidt, W. 2008, ApJ, 688, L79
Federrath, C., Roman-Duval, J., Klessen, R. S., Schmidt, W., & Mac Low, M.-M. 2010, A&A, 512, 81
Goldreich, P., & Lynden-Bell, D. 1965, MNRAS, 130, 125
Helfer, T. T., et al. 2003, ApJS, 145, 259
Jogee, S., Scoville, N., & Kenney, J. D. P. 2005, ApJ, 630, 837
Kenney, J. D. P., & Young, J. 1989, ApJ, 344, 171
Kennicutt, R. C. 1989, ApJ, 344, 685
Kennicutt, R. C. 1998, ApJ, 498, 541
Komugi, S., et al. 2005, PASJ, 57, 733
Kravtsov, A. V. 2003, ApJ, 590, L1
Krumholz, M. R., & McKee, C. F. 2005, ApJ, 630, 250
Krumholz, M. R., McKee, C. F., & Tumlinson, J. 2009, ApJ, 699, 850
Li, Y., Mac Low, M.-M., & Klessen, R. S. 2005, ApJ, 626, L823
Mac Low, M.-M., Balsara, D. S., Kim, J., & de Avillez, M. A. 2005, ApJ, 626, 864
Martin, C. L., & Kennicutt, R. C., Jr. 2001, ApJ, 555, 301
Mauersberger, R., Henkel, C., Wielebinski, R., Wiklind, T., & Reuter, H.-P. 1996, A&A, 305, 421
Murphy, T. W., Jr., et al. 1996, AJ, 111, 1025
Padoan, P., & Nordlund, A. 2002, ApJ, 576, 870
Padoan, P., Nordlund, A., & Johns, B. J. T. 1997, MNRAS, 288, 145
Pérez-Torres, M. A., & Alberdi, A. 2007, MNRAS, 379, 275
Quirk, W. 1972, ApJ, 176, 9
Reuter, H.-P., et al. 1996, A&A, 306, 721
Sakamoto, K., Baker, A. J., & Scoville, N. 2000, ApJ, 533, 149
Scalo, J., Vázquez-Semadeni, E., Chappell, D., & Passot, T. 1998, ApJ, 504, 835
Schinnerer, E., et al. 2002, ApJ, 575, 826
Schmidt, M. 1959, ApJ, 129, 243
Sofue, Y., Koda, J., Nakanishi, H., & Hidaka, M. 2003, PASJ, 55, 75
Thilker, D. A., et al. 2007, ApJS, 173, 572
Toomre, A. 1964, ApJ, 139, 1217
Vázquez-Semadeni, E. 1994, ApJ, 423, 681
Wada, K., & Norman, C. A. 2007, ApJ, 660, 276
Wang, P., & Abel, T. 2009, ApJ, 696, 96
Warren, B. E., et al. 2010, ApJ, 714, 571
Wyse, R. 1986, ApJ, 311, 41
Young, J., et al. 1996, AJ, 112, 1903